Investigation of early and late intake valve closure strategies for load control in a spark ignition ethanol engine

Author, co-author (Do NOT enter this information. It will be pulled from participant tab in MyTechZone)

Affiliation (Do NOT enter this information. It will be pulled from participant tab in MyTechZone)

Abstract

The more strict CO_2 emission legislation for internal combustion engines demands higher spark ignition (SI)engine efficiencies. The use of renewable fuels, such as bioethanol, may play a vital role to reduce not only CO_2 emissions but also petroleum dependency. An option to increase SI four stroke engine efficiency is to use the so called over-expanded cycle concepts by variation of the valve events. The use of an early or late intake valve closure reduces pumping losses (the main cause of the low part load efficiency in SI engines) but decreases the effective compression ratio. The higher expansion to compression ratio leads to better use of the produced work and also increases engine efficiency. This paper investigates the effects of early and late intake valve closure strategies in the gas exchange process, combustion, emissions and engine efficiency at unthrottled stoichiometric operation. A four-valve four-stroke single cylinder camless engine running with port fuel injection of anhydrous ethanol was employed. Early and late intake valve closure (EIVC and LIVC) strategies with a fixed maximum valve lift were compared to a conventional throttled SI valve event strategy for loads from 2.0 to 9.0 bar IMEP at 1500 rpm. The consequences and benefits to implement the unthrottled operation with each strategy were discussed. To better understand the effect of the maximum valve lift at a specific load, the valve lift was varied from 1.5 to 5.0 mm and its effects were discussed for EIVC strategy. Comparatively, the EIVC strategy presented better overall performance than the LIVC. Both unthrottled strategies provided higher engine efficiency than the conventional throttled SI strategy.

Introduction

The more strict CO_2 emissions legislation for passenger cars increased the need for more efficient spark ignition (SI) engines. Lower carbon footprint and reduced greenhouse gases (GHG) emissions are expected to reduce the climate change impacts. In this context, the use of environmentally friendly fuels with lower CO_2 emissions, such as bioethanol, has been growing worldwide. Ethanol is generally produced from fermented sugar from diverse agricultural crops. It may reduce a country oil dependency and manage surplus of agricultural crop production [1], [2]. Depending on land usage management, ethanol life cycle GHG emission can be considerably lower than that from fossil fuels[3], [4]. For this reasons, the introduction of ethanol in many countries has increased in the last decades. Even then, the international oil price, internal crop availability and sugar prices dictate the ethanol production and consumption in the larger producer countries, such as the United States and Brazil.

Ethanol has been used both as a dedicated fuel and as gasoline anti-knock additive for SI engines. In many countries, flex fuel engines permit the use of any ethanol-gasoline blend. The use of ethanol and ethanol-gasoline mixtures in SI engines has been widely reported [5]–[9]. Some ethanol advantages over gasoline are the increased knock resistance and increased heat of vaporization which may lead to higher engine efficiency. Conversely, the higher heat of vaporization decreases the engine cold start capability and the lower ethanol energy content increases the volumetric fuel consumption compared to gasoline.

In order to increase the naturally aspirated SI engine part load low efficiency, distinct strategies can be used. Lean burn and exhaust gas recirculation (EGR) may be employed to dethrottle the engine and reduce pumping losses. While lean burn highly increases the complexity of the exhaust after treatment system, EGR can be used in various ways and even enhance the after treatment system performance. In addition, the use of Miller and Atkinson cycles, based on early or late intake valve closure, can also be applied reduce pumping losses. As the intake valve closure point is moved away from bottom dead center (either earlier or later), less air is trapped in the cylinder leading to less energy released in a stoichiometric combustion. Therefore, variable valve closure strategy at wide open throttle can be used as load control method. As demonstrated in the literature, this may highly reduce the part load pumping losses while affecting the in-cylinder flow structures and turbulence levels[10]–[17].

Considering the two main large in-cylinder flow structures swirl and tumble, studies have shown that these large flow motion scales break up in small scales during the late stage of compression increasing the turbulence during combustion [18], [19]. The tumble motion is the large scale fluid motion generated during the intake stroke around an axis perpendicular to the cylinder center line. While the piston is moving towards TDC, during compression, the tumble motion initially increases due to angular momentum conservation. Later, during compression stroke, the large flow structure is distorted due to wall shear stress and decays in smaller turbulence structures[20]–[22]. Swirl is the rotational fluid motion around the cylinder axis. Conversely to tumble, the swirl motion is less affected by wall friction and hence its angular momentum can be well sustained until the end of the compression stroke [23]. So, in four-valve SI engines with symmetric configuration, the increase of the tumble in-cylinder motion is expected to generate higher turbulence levels prior to combus-

tion than the increase in swirl [24], [25]. Even then, if not enough tumble motion is generated e.g at mid-low engine loads, poorer turbulence levels are obtained [26].

Conventionally, swirl has been used in two valve SI engines and diesel engines, while tumble has been preferential for four valve engines due to valve cylinder head symmetry aspects. Swirl generation is rather difficult at such conditions without deteriorating flow performance. The use of such in-cylinder flow motion is of major importance for lean burn engines, where the laminar speed is lowered and the flow field has more time to distort the flame until the end of combustion [27]. Also, the flow field directly affects the in-cylinder heat transfer, and as swirl is maintained during the combustion process, extreme fluid motion may decrease engine overall efficiency[23], [28].

The use of early intake valve closure (EIVC) strategy has shown to promote an initial increase in tumble motion near BDC. If the flow motion is not strong enough, the tumble structure may breakdown in the middle of the compression stroke generating lower turbulence levels than the conventional throttled operation [14] [16]. In the other hand, the use of late intake valve closure (LIVC) is expected to maintain similar turbulence levels or even increase them compared to a conventional intake valve closure timing [29].

Lately, with the availability of various valve train solutions such as simpler cam phasing mechanisms to fully variable valve trains, the use of EIVC and LIVC concepts have become more usual. Several systems still use the throttle in order to facilitate load control and only a small number have full valve timing and lift capability. Even then, there is still the question regarding which strategy would be the best in a fully variable valve train scenario for a naturally aspirated engine.

Thus, the objective of this work was to identify which of the load controlling strategies through intake valve closure (LIVC or EIVC) result in better fuel economy for unthrottled stoichiometric SI operation with ethanol at low engine speeds. The investigation was focused on the gas exchange process and its effects on combustion and engine out emissions. As the test engine had fully variable capability, the influence of the maximum intake valve lift was also investigated to evaluate its effect on engine operation for the best load control strategy.

Experimental setup

The engine used in the experiments was a camless four valve single cylinder SI research engine. The camless system is based on electro-hydraulic valve actuators that enabled independent valve timing and lift control [30], [31]. The tests were conducted with port fuel injection (PFI). The spark and injection timings, as well as valve parameters, were controlled using a Ricardo rCube engine control unit (ECU). Table 1 presents the engine specifications and Figure 1 presents the test cell setup.

The engine was coupled to an AC dynamometer which enabled motoring and firing tests. The engine test cell had closed loop coolant and oil temperature control, both maintained at 363 K. An Endress+Hauser Promass 83A Coriolis meter was used to measure fuel flow rate. Intake air mass flow rate was measured by a Hasting HFM-200 laminar flow meter. Intake air temperature was kept at 303 ± 5 K. The in-cylinder pressure was measured by a Kistler 6061B piezoelectric sensor. Intake and exhaust pressures were measured by Kistler piezoresistive absolute pressure sensors 4007BA20F and 4007BA5F, respectively. An encoder with 720 pulses per revolution, directly connected to the crankshaft, was used to relate the pressure data to the crank angle. K-type thermocouples were used to collect average temperatures at relevant locations, such as intake and exhaust manifolds, oil and coolant galleries, fuel rail, and valvetrain oil supply. An in-house high speed data acquisition and combustion analysis system was used to monitor and record all parameters. Fuel temperature was maintained at 298 ± 5 K and injection pressure was held at 3.5 ± 0.25 bar. The twin spray PFI injector was installed in the intake runner before the intake ports. Each fuel spray cone was targeted to one of the intake ports. Anhydrous ethanol (99.1 % v/v ethanol-in-water) was used as fuel.

Table 1. Engine characteristics

Engine model	Ricardo Hydra Camless Two/four-strokes
Displaced volume	350 cm^3
Bore	81.6 mm
Stroke	66.9 mm
Compression ratio	11.8:1
Combustion chamber	Four valves pent-roof with central spark plug
Fuel	Anhydrous ethanol (E100)
Port fuel injector	Twin spray Bosch EV 14

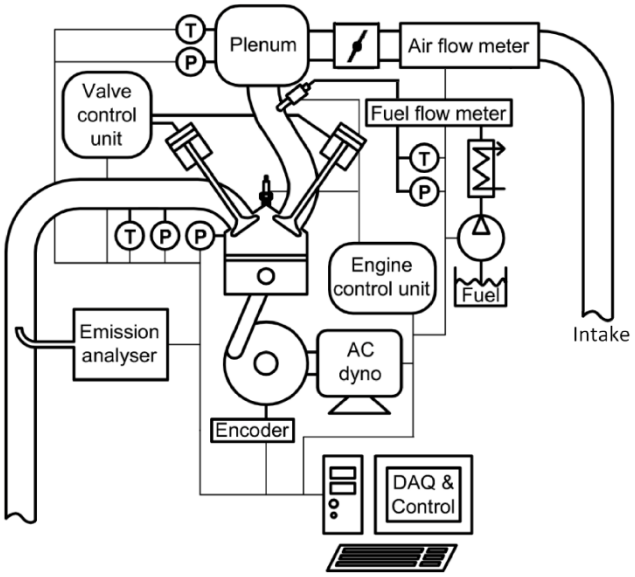

Figure 1. Schematic representation of the engine test cell.

The heat release analysis was calculated based on the first law of thermodynamics:

$$\frac{dQ_{net}}{d\theta} = \frac{\gamma}{\gamma-1} p \frac{dV}{d\theta} + \frac{1}{\gamma-1} V \frac{dp}{d\theta} \quad (1)$$

This equation correlates the apparent heat release Q_{net} (which is the sum of instantaneous fuel heat release due to combustion and in-cylinder heat transfer) to the cylinder work and variation of charge internal energy, using the instantaneous in-cylinder pressure (p) and

combustion chamber volume (V), and their changes related to the crank angle θ. Gamma (γ) is the ratio of specific heats.

Carbon monoxide (CO), hydrocarbons (HC) and oxides of nitrogen (NOx) emissions were measured using a Horiba MEXA-7170 DEGR analyser. As it is known, a considerable part of unburned organic gaseous emissions is constituted by aldehydes and unburned ethanol in addition to hydrocarbons when the engine is fuelled with ethanol[32], [33]. It is thus important to correct the flame ionization detector (FID) outputs for its lower response to the organic unburned species containing oxygen to carbon bonds. A correction factor k_{FID} was applied to the raw FID_{ppm} measurement depending on the ethanol volumetric content (e) in the fuel [34], [35]. The correction factor methodology was presented by Kar et al.[34] and the correction constants of 0.60 and 0.68 for the FID response towards acetaldehyde and ethanol, respectively, were proposed by Wallner et al.[35]. A singular response factor of 0.64 was used in this study, as it represents the average between the response factors of such species. The nomenclature "total hydrocarbons" (THC) was used to represent the corrected unburned organic emissions. Thus, the corrected FID measurement THC_{ppm} and its correction factor k_{FID} were calculated as follows:

$$THC_{ppm} = FID_{ppm} * k_{FID} \quad (2)$$

$$k_{FID} = \frac{1}{1-(1-0.64)(0.608e^2+0.092e)} \quad (3)$$

For anhydrous ethanol the calculated k_{FID} was 1.34.

The procedures presented in the EU Emission Regulation[36] were followed for the calculations of the indicated specific emissions as well as for the conversion of CO and NOx from dry to wet basis. The indicated specific gaseous emissions of each exhaust components evaluated ($ISgas_i$) were calculated by:

$$ISgas_i = \frac{u_i\,[x_i]\,k_w\,\dot{m}_{exh}}{P_I} \quad (4)$$

where u_i and $[x_i]$ are the raw gas exhaust factor[36] and the concentration (in ppm) of the i chemical element in the exhaust flow, respectively; k_w is the dry to wet correction factor applied to CO and NOx; $\dot{m}_{exh}$ is the exhaust mass flow rate calculated as the sum of the instantaneous fuel and air mass flow rates; P_I is the indicated power.

Test methodology

Initially, tests were carried at 1500 rpm at loads of 2.1 bar, 3.1 bar, 4.5 bar, 6.1 bar, 7.5 bar and 9.0 bar ± 0.1 bar IMEP in order to compare the conventional throttled SI (tSI) operation to early and late intake valve closure load control methods. The intake valve opening, and exhaust valve closure and opening points were kept fixed during all tests. The overlap between intake and exhaust valves could be considered null as it was around 2 CAD with 0.2 mm valve lift. For this reason, the residual gas fraction could be maintained fairly constant for all load control strategies at each load. This way, the impact of the IVC moment in the engine operation could be directly assessed.

An example of the actual intake valve lift profile used at 3.1 and 6.1 bar IMEP load with each load control strategy is presented in Figure 2. For the tSI method the intake valve profile was kept constant and the load was controlled using a conventional throttle. For the EIVC and LIVC, the load was controlled by advancing or delaying the IVC with wide open throttle. Intake and exhaust valves maximum lifts were kept constant at 3.0 mm target. This value was used to provide the same valve flow restriction while excluding the effect of the valve lift, and for safety reasons (at this lift the valves cannot hit the piston). The studies did not aim to show a valve timing optimization in the context of maximizing the engine efficiency. They were designed to specifically show the IVC impact in the engine operation parameters according to the chosen load control strategy.

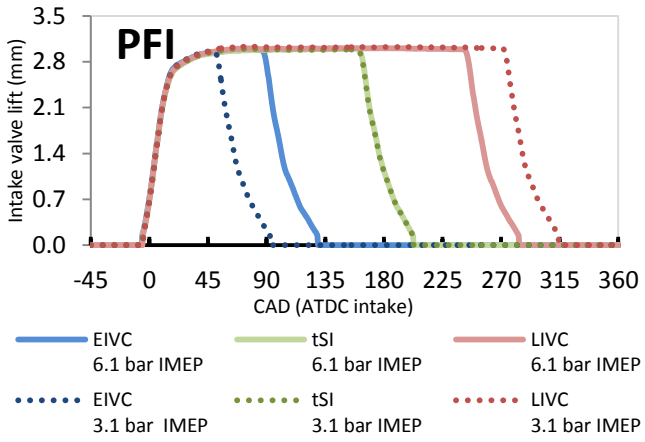

Figure 2. Intake valve lift profiles of 3.1 and 6.1 bar IMEP loads for different load control strategies and PFI injection strategy.

PFI injection timing was set to firing TDC in order to provide the maximum time for ethanol vaporization and mixing with air. Spark sweeps with 2 CAD increment were run at each operating point in order to find the minimum spark advance for the best torque (MBT).

Later, EIVC tests were conducted only at 3.1 bar and 6.1 bar IMEP and 1500 rpm with different maximum valve lifts of 1.5 mm, 2.0 mm, 3.0 mm, 4.0 mm and 5.0 mm. This way the effect of the maximum valve lift in the engine operating parameters could also be assessed.

Results

Comparative analysis between tSI, EIVC and LIVC

Gas exchange analysis

Figure 3 presents the IVC event necessary to achieve different loads for each strategy and the resultant geometric and effective compression ratios (CR_v and CR_p, respectively). Second and third order polynomial curve fitting were used to connect the data points in the plots for better visualization purpose. In the case of conventional throttled operation, the restriction on the amount of air was provided by the closure of the throttle. In the case of EIVC or LVIC, the amount of air trapped in the cylinder was a function of the instantaneous in-cylinder volume at IVC whilst the intake manifold pressure was near to atmospheric condition. For this reason, in order to reduce the load, the IVC event had to be advanced or delayed from the BDC for the EIVC and LIVC strategies, respectively.

As the IVC was varied, the geometric compression ratio, CR_v, deviated from the geometric compression ratio determined by the cylinder volumes at BDC and TDC. CR_v was calculated as the relationship between the TDC in-cylinder volume and volume at IVC. Very low

CR_v values were achieved at the lowest loads when using the LIVC strategy. This occurred because the cylinder volume required to trap the amount of air was too small. Due to the valve restrictions and higher in-cylinder pressure required to dispose the excess air back to the intake manifold, an earlier compression phase occurred previously to the IVC event, as shown in Figure 4. Thus, for the LIVC strategy the CR_v was always smaller (for all loads) than the CR_p. The CR_p was calculated as the relationship between the instantaneous in-cylinder volume when a fitted polytropic compression process (fitted to the compression process while all valves were closed) reaches the intake pressure level and combustion chamber volume. Using this approach, the CR_p means the actual compression ratio to which the fluid is subjected starting at the intake pressure state. Figure 4 provides the graphical explanation of the calculation process of CR_p and CR_v.

Because of the reversed flow associated with the very late IVC during the compression stroke, at the 2 bar IMEP load, LIVC operation with WOT could not be achieved as the IVC had to be delayed to near to the TDC resulting in very low compression. As mentioned in [16], [11], this would require a spark advance before the IVC in order to increase peak in-cylinder pressure and temperature for stable combustion. For this reason, intake throttle was used to reduce intake manifold pressure to 0.9 bar when operating at 2 bar IMEP and LIVC.

In the case of EIVC, the flow restrictions during the valve closure event started an over-expansion phase before the IVC event. Thus, the CR_p of the EIVC cases was always lower than the it's CR_v.

Another point to be addressed to the LIVC characteristics is the pumping loss associated to the longer flow period while the intake valves were still opened, as shown in Figure 5. Ideally, for adiabatic and reversible flow processes, when the piston reached the BDC, the in-cylinder pressure would be equalized to the intake manifold pressure. During the initial compression phase, while the intake valves were still opened, the in-cylinder pressure would be just slightly higher than the intake pressure in order to promote the required in-cylinder charge backflow.

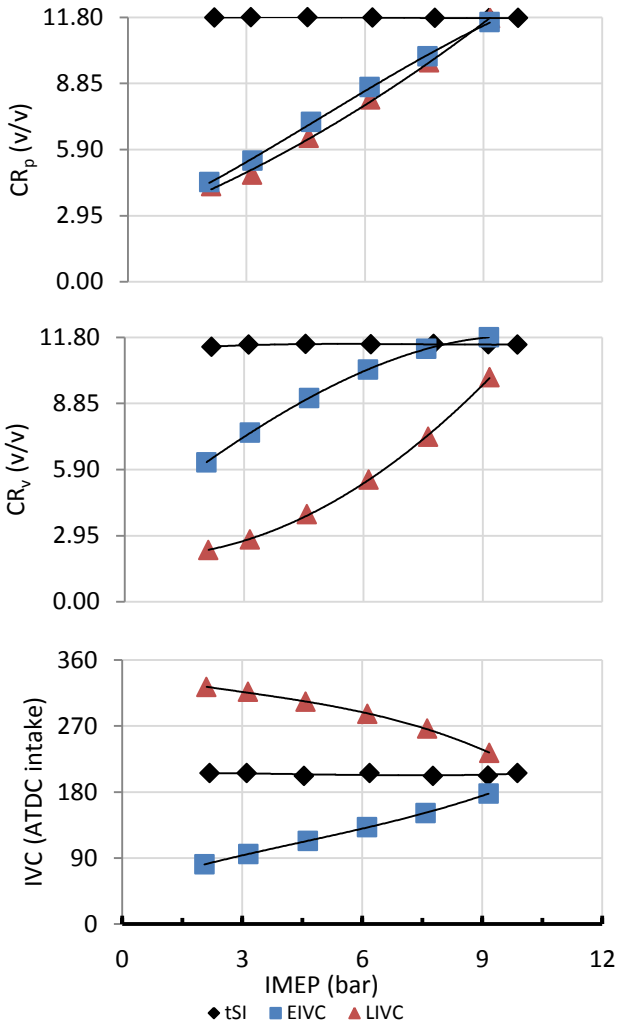

Figure 3. Effect of the load control method in the intake valve closure timing, geometric compression ratio CR_v and effective compression ratio CR_p.

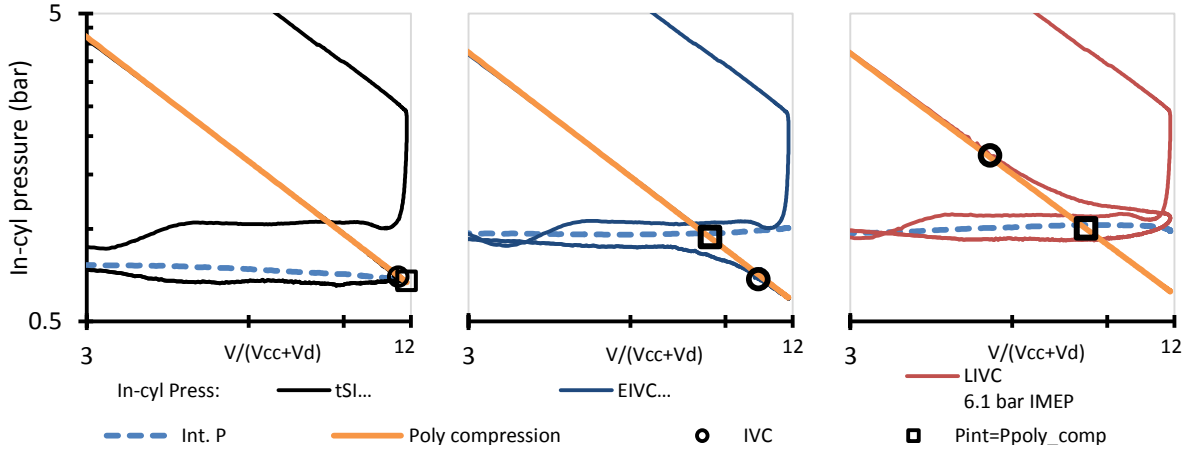

Figure 4. Effect of the load control method in the pumping loop of 6.1 bar IMEP load – Log P x Log V plots with in the intake valve closure and the effective compression ratio .

In reality, due to the valve flow restriction and to overcome the momentum of the fluid, the in-cylinder pressure increased to higher levels than ambient pressure. The flow losses would be increased in the LIVC case due to the longer period with the intake valves opened, as also stated by [10]. The increased flow losses occur due to the additional backflow process necessary to trap the right charge mass quantity for the desired load. Thus, for the LIVC strategy, valve flow restrictions needed to be surpassed twice in the fresh air trapping event (during the fresh air induction and in the subsequent backflow processes).The early compression phase reduced the total available work from the power strokes and affected the PMEP. This work is represented by the purple delimited area in Figure 5.

For the EIVC strategy the valve flow restriction needed to be surpassed only during a minimized period during the fresh air induction process while the intake valves were opened. Nevertheless, the valve flow restrictions increased the over-expansion pumping loop work at some extent during the intake valve closing phase (delimited by the purple perimeter in Figure 5). Ideally, the over-expansion period would only begin at the IVC following a polytropic compression behavior. Despite this, a major part of the over-expansion phase work (delimited by the green area) was recovered in the compression phase until the in-cylinder pressure was equalized to ambient pressure. For these reasons, EIVC PMEP work was smaller than LIVC PMEP.

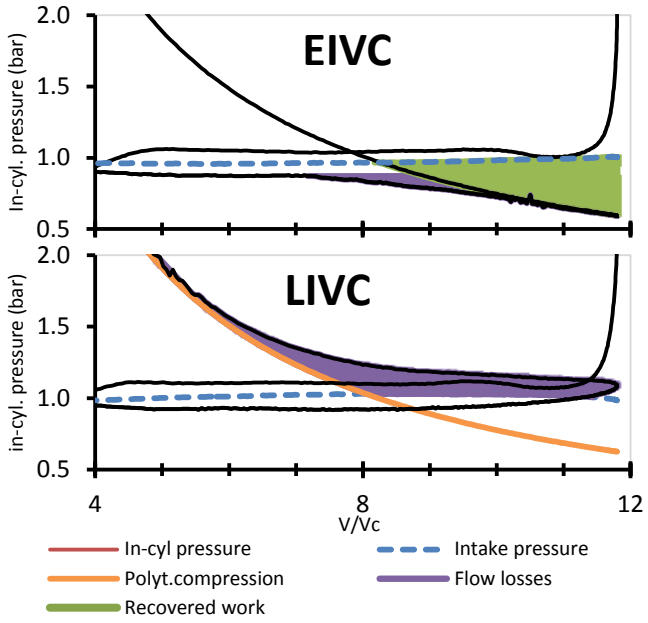

Figure 5. LogPxLogV plot with emphasis in the flow losses of the EIVC and LIVC load control strategies – 6.1 bar IMEP.

In the tSI cases, the lower plenum pressure due to partially closed throttled created a considerable difference between in-cylinder pressure and ambient pressure during the intake phase. This resulted in the larger PMEP.

The variation in pumping work was directly translated to gas exchange efficiency, shown in Figure 6. Gas exchange efficiency calculation and physical meaning is explained in Appendix A. For the tSI strategy and at the lowest loads, almost 25% of the energy produced in the engine was used to overcome the pumping work. The increased flow losses during the backflow period of the LIVC strategy decreased its gas exchange efficiency as the load was reduced.

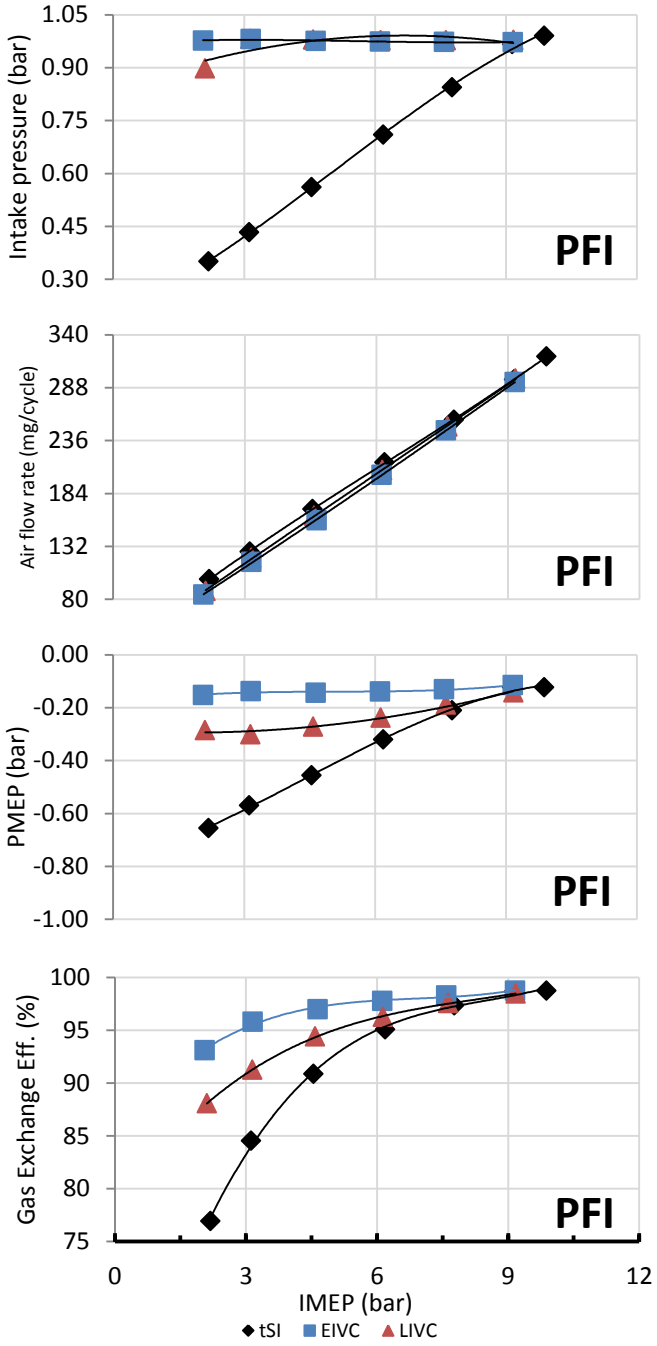

Figure 6. Effect of the load control method in the intake pressure, air flow rate, pumping mean effective pressure and gas exchange efficiency at different loads.

If only the gas exchange work would be considered, more energy would be consumed in as pumping work (more negative PMEP) in the tSI. Thus, for stoichiometric combustion, more air was required in order to provide the same load. Thus, the low load EIVC and LIVC presented similar air flow rate while tSI presented the highest. As load increased and the difference between each strategy pumping losses decreased, the air flow rate tended to be equalized.

Combustion characteristics

Conventional spark ignition combustion dominated by flame propagation occurred in all tested scenarios. Combustion phasing was controlled through spark timing, and MBT operation could be achieved without knock. Figure 7 presents the required spark timing for MBT and the point where 50% of the mass was burnt (CA50%). The spark timing required for the different strategies was a function of load and initial compression temperature. In the EIVC strategy, the in-cylinder temperature prior to the spark was lower than in the tSI cases due to reduced compression period (lower compression ratios). This effect required a higher spark advance in order to correctly phase the combustion. As the load increased, the over-expansion period was reduced and the CR_p increased. This enabled the use of more retarded spark timing. In the tSI case, the required spark advance slightly increased with the load. This effect could be attributed to higher turbulence levels as load increased. The combustion phasing general trend was in accordance to the literature: the longer the combustion, the more delayed was the CA50% from the TDC [37]. The in-cylinder temperature prior to spark e and at -35 CAD ATDCfiring for the 3.1 bar and 6.1 bar IMEP PFI cases are plotted in Figure 8. The effects of the valve strategy in the flame development angle (FDA – period between spark and 10% of mass fraction burn), main phase combustion duration (10-90MFB – period between 10% and 90% of mass fraction burned) and cycle-to-cycle variability of the IMEP (COV_{imep}) are shown in Figure 9.

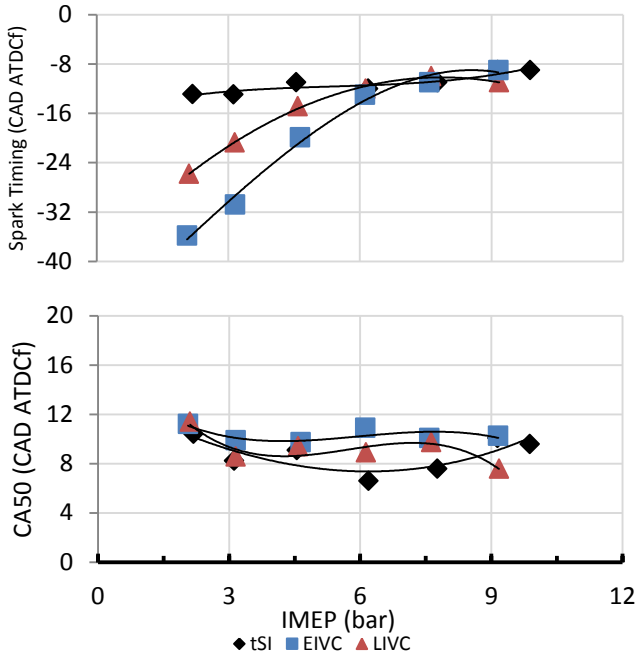

Figure 7. Effect of the load control strategy in spark timing and CA50% at different loads.

It should be considered that each strategy generated different large flow motion structure intensities which decayed to different level of turbulence prior to spark. Summed to this, the in-cylinder pressure and temperature also played a major role affecting the flame speed. Thus, EIVC strategy presented both longest FDA and combustion duration. This could be explained by the expected lower in-cylinder temperature and low turbulence levels near the spark plug prior to ignition.

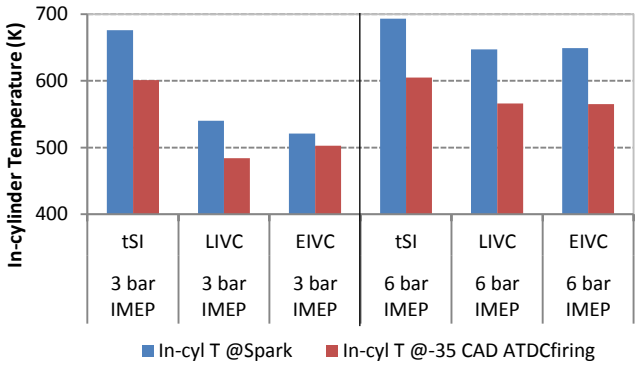

Figure 8. Effect of load control method in the in-cylinder temperature at -35 CAD $ATDC_{firing}$.

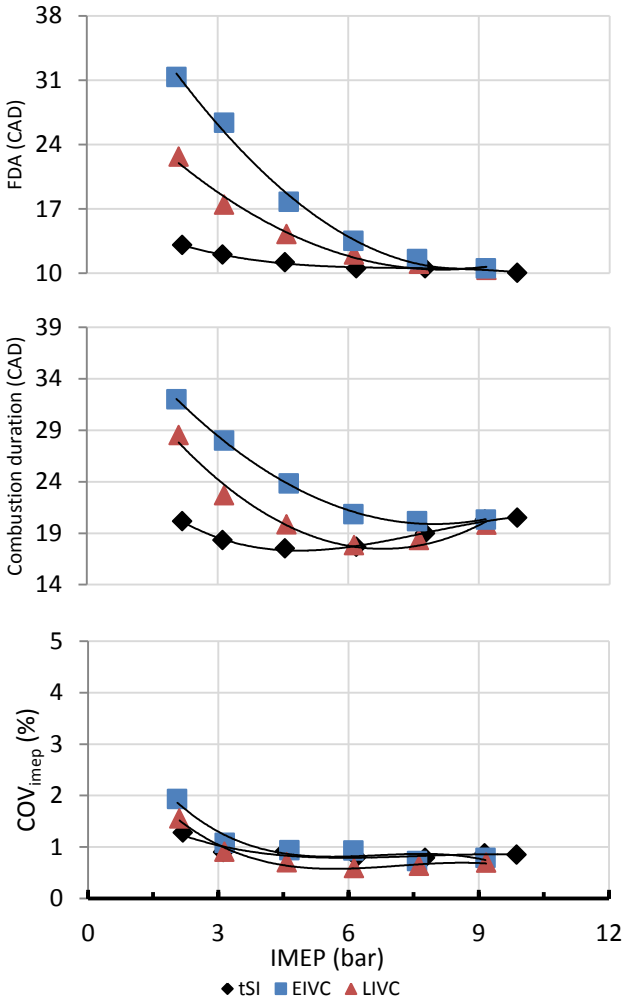

Figure 9. Effect of the load control method in flame development angle, combustion duration and COV_{imep} at different loads.

As shown elsewhere [38], in the period right after spark, the initial flame development stage is governed by the thermodynamic state of the charge and mixture composition near the spark plug (which was expected to be homogeneous due to the PFI strategy). After an initial growth period, the interaction between the flame front and the turbulent eddies start. Flame front corrugation and wrinkling increase the flame front area. Due to the reduced size of the flame kernel, the

largest eddies in the flow can convect it from the spark plug electrode. Later, during the turbulent flame propagation stage, the mean velocity field and local air/fuel ratio play a minor role in the main combustion duration, as a number of local events are averaged for the final effect. According to this, it could be expected that the earlier the IVC, not only the lower was the CR_p and in-cylinder temperature but also the turbulence levels. As load increased and the IVC became closer to the BDC, a more stable tumble structure was expected. This structure would last until the end of the compression stroke resulting in higher turbulence levels which helped in the flame propagation process.

The lower LIVC CR_p decreased the pressure prior to spark to the same levels of the EIVC case. This resulted in lower temperature prior to combustion and longer FDA and combustion duration when comparing LIVC to tSI. Even then, the turbulence levels were expected to be higher with the LIVC than the EIVC.

It could be concluded that the considerable increase in the duration of the whole combustion process for the EIVC strategy at low loads occurred mainly due to poor in-cylinder flow motion and low turbulence levels. This conclusion was supported by the fact that the LIVC case presented even lower compression temperature than the EIVC case (comparing the in-cylinder temperatures of the 3.1 bar IMEP cases presented in Figure 8) but still provided a faster combustion process. Similar results comparing EIVC, LIVC and tSI at low load were reported elsewhere[17]. Even though the duration of the combustion was longer in the unthrottled cases, the COV_{imep} could be kept below 2% with the aid of distinct spark timing

The instantaneous averaged in-cylinder pressure and heat release rates of 3.1 bar and 6.1 bar IMEP of all load control strategies are presented in Figure 10. For the longer combustion durations cases, the peak in the heat release rate decreased and was delayed from the TDC. The same behavior occurred to the peak of the pressure of the averaged pressure data cycle (of 100 cycles). The resultant maximum in-cylinder peak pressure was fairly the same for both unthrottled strategies, with slightly higher results for the tSI strategy, as shown in Figure 11. The exhaust temperature of the EIVC was the higher due to the considerably longer combustion duration.

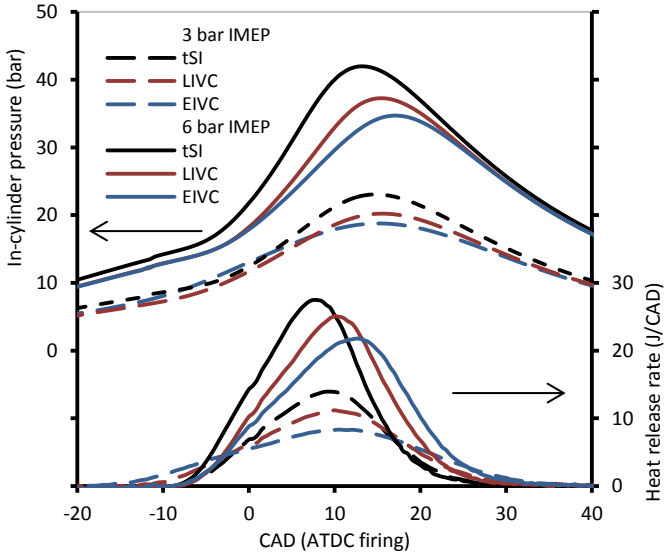

Figure 10. Average in-cylinder pressure and heat release rate of different valve strategies for 3.1 bar and 6.1 bar IMEP loads.

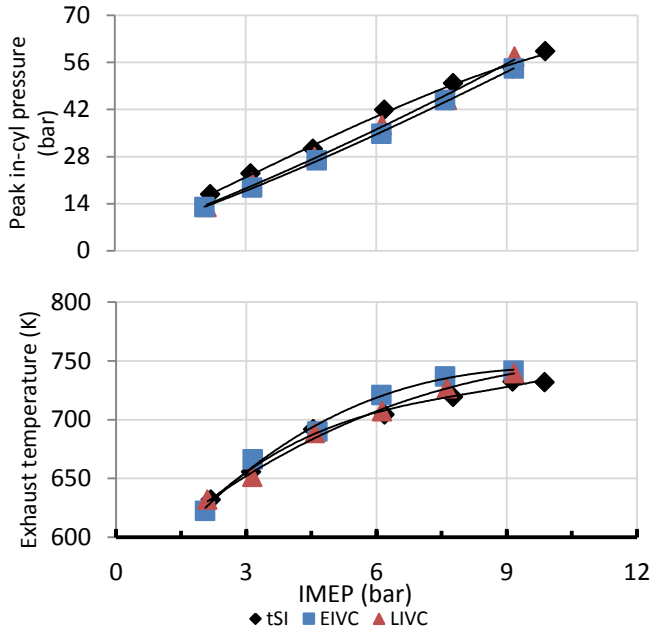

Figure 11. Effect of the load control method on maximum in-cylinder pressure and exhaust temperature for different loads.

Gaseous emissions

Figure 12.presents the gaseous emissions of the different load control strategies at different loads. A major trend of decrease in CO and THC emissions with the increase in load was found for all strategies. This occurred because at higher loads, the higher combustion temperatures increased the ethanol breaking into smaller species and the oxidation process of such species.

The CO formation was not expected to be a result of locally fuel rich areas as the homogeneity level achieved with PFI was expected to be the same for all conditions. Even then, as CO formation is primarily dominated by air-fuel ratio and temperature, the small ISCO differences between cases could be attributed to different combustion temperatures and small deviations from the target stoichiometric lambda (as lambda control was manual).

The THC emissions are affected by combustion chamber design and mixture formation process, and combustion temperature and post oxidation after the main combustion phase. The cause for the lower THC emissions in the EIVC case would be the longer combustion duration which increased the temperature during the expansion phase and increase the post combustion oxidation process.

As expected, NOx emissions increased with the load occurred. This occurred due to the temperature influence in the NOx formation, explained by the Zeldovich mechanism. The lower NOx specific emission of the EIVC and LIVC cases was a direct evidence of lower combustion temperatures. The pressure levels during EIVC combustion were lower than the LIVC ones and consequently the expected combustion temperatures would be lower. Even then, the NOx emissions of the EIVC and LIVC were virtually the same. This could be explained by the increased period which the mixture was exposed to the high flame temperature due to the considerably longer combustion durations. The increased timed for the NOx formation would compensate the lower combustion temperatures.

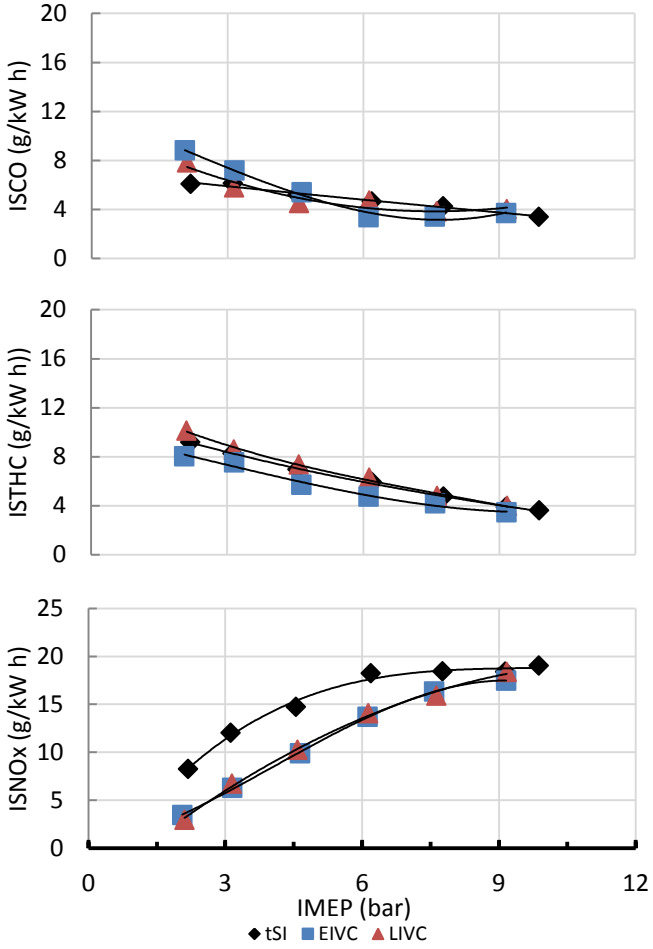

Figure 12.Engine out emissions for the different load control methods and loads.

The use of a conventional SI after treatment system based on a three-way catalyst would be enough to handle exhaust emissions for the variable IVC load control strategies considering the stoichiometric combustion and the exhaust gas temperatures which were always higher than 600 K.

Efficiency related parameters

The gaseous exchange efficiency, the main reason for the low part load SI efficiency, was previously discussed and shown in Figure 6. Even then, it is worth to highlight that EIVC provided the highest gas exchange efficiency, followed by the LIVC. The conventional throttled operation provided the lowest gas exchange efficiency. Added to the gas exchange efficiency, it is important to evaluate the combustion and thermodynamic efficiencies to understand all the effects that affected the indicated efficiency of each strategy. These parameters are shown in Figure 13. The calculation procedure used to calculate the efficiency related parameters is provided in appendix A.

The combustion efficiency which is related to fraction of fuel mass energy released during the combustion process could be related to CO and THC emissions. The better combustion efficiency levels were achieved at higher loads, where the emissions were the lowest. Due to the slightly lower EIVC part load THC emissions (which has the major impact in the combustion efficiency), these operation conditions provided the highest combustion efficiency.

The gross thermodynamic efficiency was calculated in order to assess the efficiency of the engine to convert the heat released during the combustion process into work. As all the operating points were run at MBT, the best combustion phasing which would increase the engine thermodynamic efficiency was achieved. So, the major difference in thermodynamic efficiency is related to how well the combustion occurred for each strategy, the relationship between produced power and consumed power, and the in-cylinder heat transfer losses. As thermodynamic efficiency cannot be directly measured, it was assessed through the relationship between net indicated efficiency to combustion and gas exchange efficiencies. At the lowest loads (2 and 3.1 bar IMEP) the long combustion process of the EIVC and LIVC strategies degraded the thermodynamic efficiency. For loads higher than 4.5 bar IMEP the lower combustion temperature reduced combustion heat transfer at a relatively faster rate increasing the thermodynamic efficiency to higher than tSI levels. Increased in-cylinder heat transfer could be one of the reasons for the slightly lower thermodynamic efficiency of LIVC strategy compared to the EIVC strategy. This would occurs due to the backflow of the charge before the IVC which cooled the cylinder walls and increased the heat losses [17].

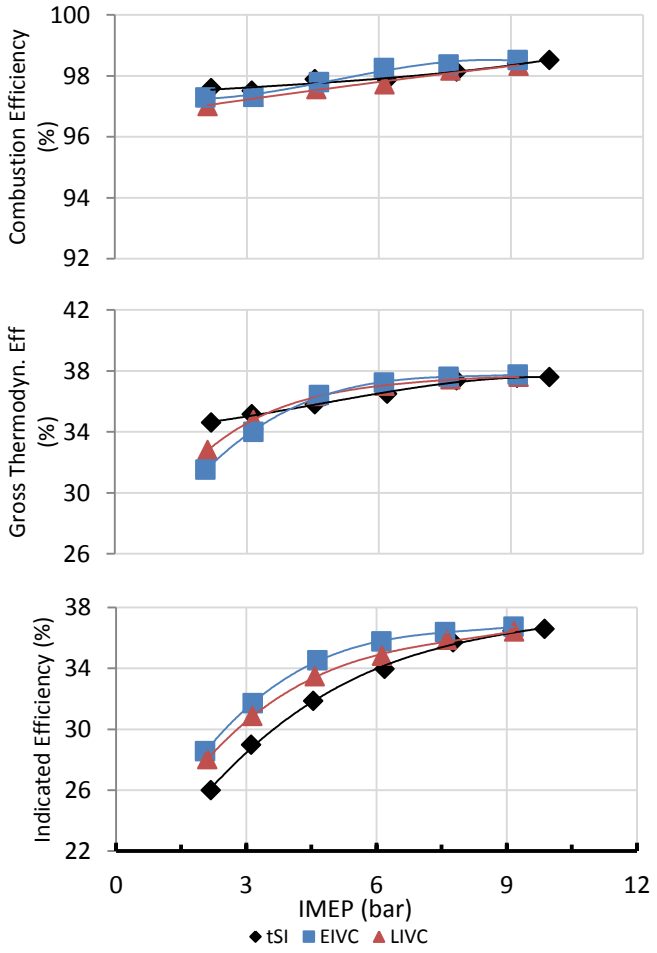

Figure 13. Efficiency related parameters for different load control methods and loads.

In the case of the LIVC, the relationship between work produced during the power strokes and gas exchange strokes was smaller. Although this strategy presented the lowest pumping losses, the early compression phase flow losses reduced the power strokes to pumping

strokes work relationship. As the load increased and the IVC was closer to the BDC, the heat losses would be reduced, effective compression ratio increased, and the thermodynamic efficiencies would be equalized to the tSI case.

The indicated efficiency was calculated from the relationship between the in-cylinder gas work (from the pressure-volume diagram) and the total fuel energy delivered to the engine in one cycle. It can be explained as a result of the relation of three previously discussed efficiencies. EIVC resulted in the higher indicated efficiency for all loads. For the lowest loads the comparatively smaller pumping work (compared to other strategies) and the good combustion efficiency counter balanced the lowest thermodynamic efficiency.

The good thermodynamic combustion heat release process of the LIVC strategy was counter balanced by average gas exchange efficiency and the lowest combustion efficiency. This resulted in intermediary net indicated efficiency compared to the other strategies, slightly lower than EIVC but considerably higher than the tSI net indicated efficiency.

The tSI case presented the lowest net indicated efficiency especially due to the impaired gas exchange efficiency. If directly translated to real world operation, the unthrottled operation indicated efficiency gains would result in better fuel economy. Thus, it could be expected around 3.7% or 5.9% fuel economy gain when using LIVC or EIVC, respectively, against the conventional tSI (when averaging the net indicated efficiency gains for all loads). Considering only the loads up to 4.5 bar IMEP, the average gain would be 6.5% and 9.2% (for LIVC and EIVC strategies, respectively).

Effect of maximum valve lift in EIVC unthrottled operation

Gas exchange analysis

As the EIVC strategy showed better potential in increasing SI engine efficiency than LIVC a second study was performed in order to understand the effects of the maximum valve lift in the engine operation. For this study, the investigations were carried at the loads of 3.1 bar and 6.1 bar IMEP at 1500 rpm. The target maximum valve lifts used were: 1.5 mm, 2.0 mm, 3.0 mm, 4.0 mm and 5.0 mm. Wide open throttle was used and the load was controlled by the IVC moment. Figure 14 presents the resultant intake valve lift profiles used in the tests.

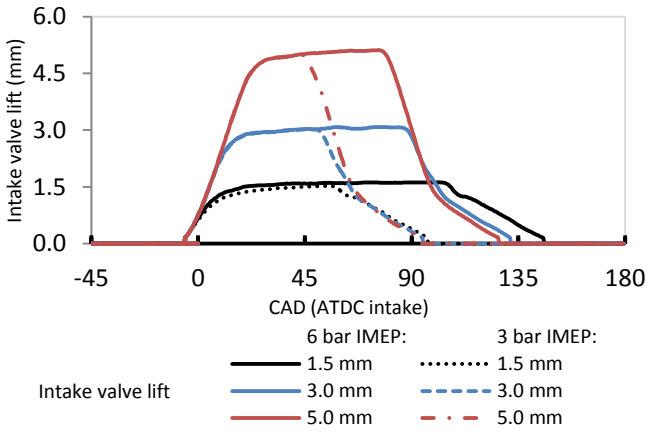

Figure 14. Intake valve lift profile for different maximum intake valve lifts and loads.

The EIVC had to be adjusted depending on the set maximum valve lift in order to maintain the desired load. Figure 15 presents the required IVC and the calculated CR_v and CR_p. As the valve lift was increased, the IVC had to be advanced nearer to the TDC because the flow curtain area proportionally increased with the maximum valve lift and the air flow was facilitated. In order to maintain almost the same amount of trapped air (to maintain the same load) a smaller intake valve opening period was necessary when increasing the valve lift. It should be pointed that as the valve lift increases the discharge coefficient (Cd) related to the curtain area decreases [39].So, at a higher lift, the relation between the actual flow rate and the isentropic flow rate is smaller than that of lower valve lifts. This effect occurs because of the flow dynamics and detachment of the boundary layer in the valve seat and back of the valve. Thus, the flow area at higher lifts resulted in a relatively higher flow restriction than that from the lower lifts. For this reason the IVC trend against valve lift was not linear as would be according only to the curtain area. Also, as the load increased, the period which the flow was subjected to a higher valve lift (with higher Cd) increased. This resulted in a higher IVC difference between the maximum and minimum lifts for the 6 bar IMEP.

The effect of the IVC in the CR_v was higher than in the CR_p. At lower lifts, even though the Cd was higher, the flow was more restricted by the reduced curtain area decreasing the in-cylinder pressure prior to the start of the valve closure period. Thus, even with a later intake valve closure, the minimum pressure of all lifts for the same load was almost the same and the compression pressure was almost the same for the same CAD. This resulted in an almost constant CR_p behavior.

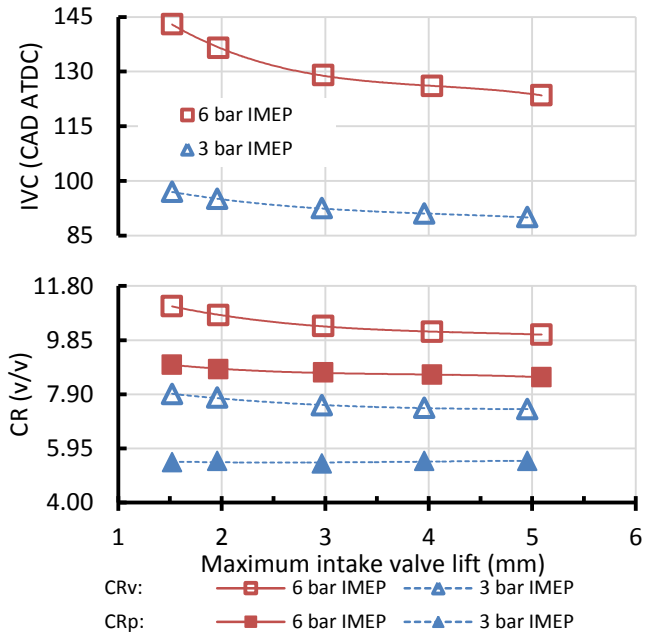

Figure 15. Effect of maximum intake valve lift in the IVC and effective and geometric compressioratios.

As the pressure difference between the intake and exhaust stroke increased (due to reduced area at lower valve lifts), the pumping work also increased (the higher the consumed work during the pumping loop the more negative was the PMEP). Figure 16 presents the pumping loop of three different lifts for the 3.1 bar and 6.1 bar IMEP loads and Figure 17 presents the pumping mean effective pressure and gas exchange efficiency for the different maximum valve lifts

and loads. The decrease in the PMEP directly reflected the gas exchange efficiency which was enhanced as the valve lift was increased. The absolute gain in the gas exchange process was 1.3% and 2.0%, for the 3.1 bar IMEP and 6.1 bar IMEP respectively.

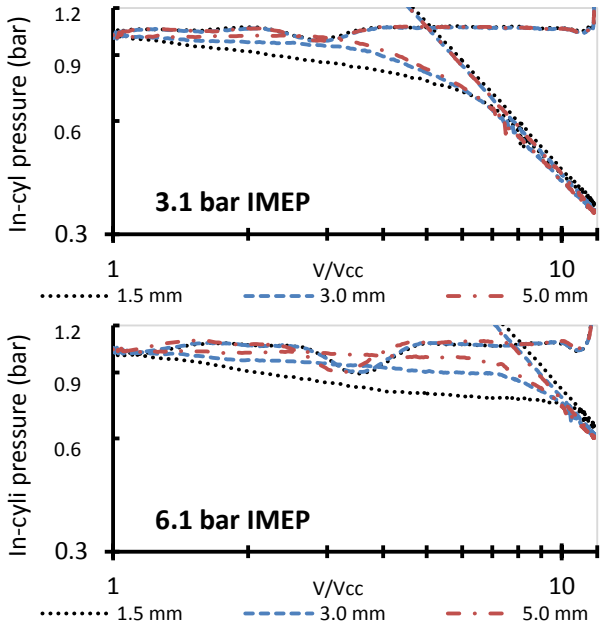

Figure 16. Effect of maximum valve lift in the pumping loop.

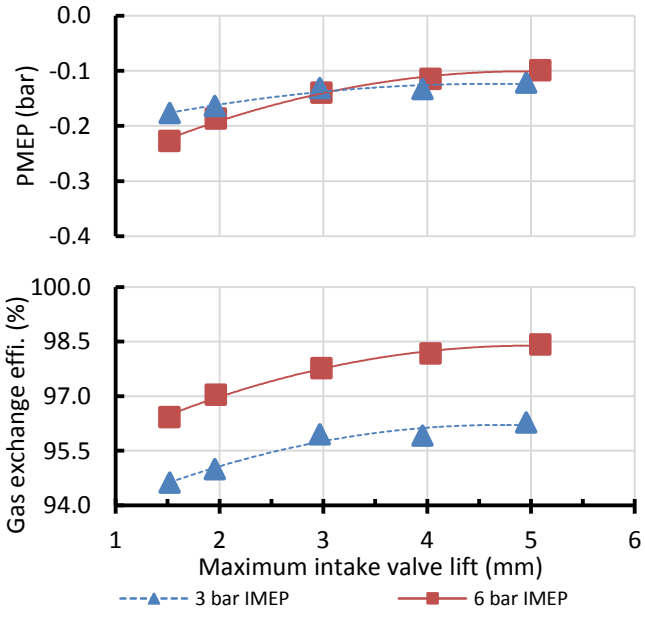

Figure 17. Effect of maximum valve lift in PMEP and gas exc. efficiency.

Combustion characteristics

Spark timing, flame development angle, combustion duration and COV_{imep} are presented in Figure 18. MBT could be achieved in all operation conditions and conventional spark ignition combustion occurred. The less advanced spark timing occurred for the lowest lift but there was no recognizable trend between spark timing and maximum intake valve lift. Even with the delayed spark timing in the

lowest lift case the FDA and combustion duration were the lowest. There was an increasing trend for the FDA and combustion duration as valve lift increased. One possible explanation for this would be that for lower valve lifts there was higher in-cylinder flow motion and turbulence generated by higher velocity of the air flow jets through the reduced valve curtain area. This trend was in agreement with [13], which stated that higher in-cylinder flow motion and turbulence could be achieved using low valve lift profiles at the cost of higher pumping losses.

Another parameter that helped to reduce the combustion process duration was the CR_p. Even though the variation of CR_p with the maximum valve lift was small, it could be seen from Figure 16 that the compression occurred at slightly higher pressure for the lowest valve lifts. This resulted in small temperature increment prior to spark which would enhance the combustion process in low loads.

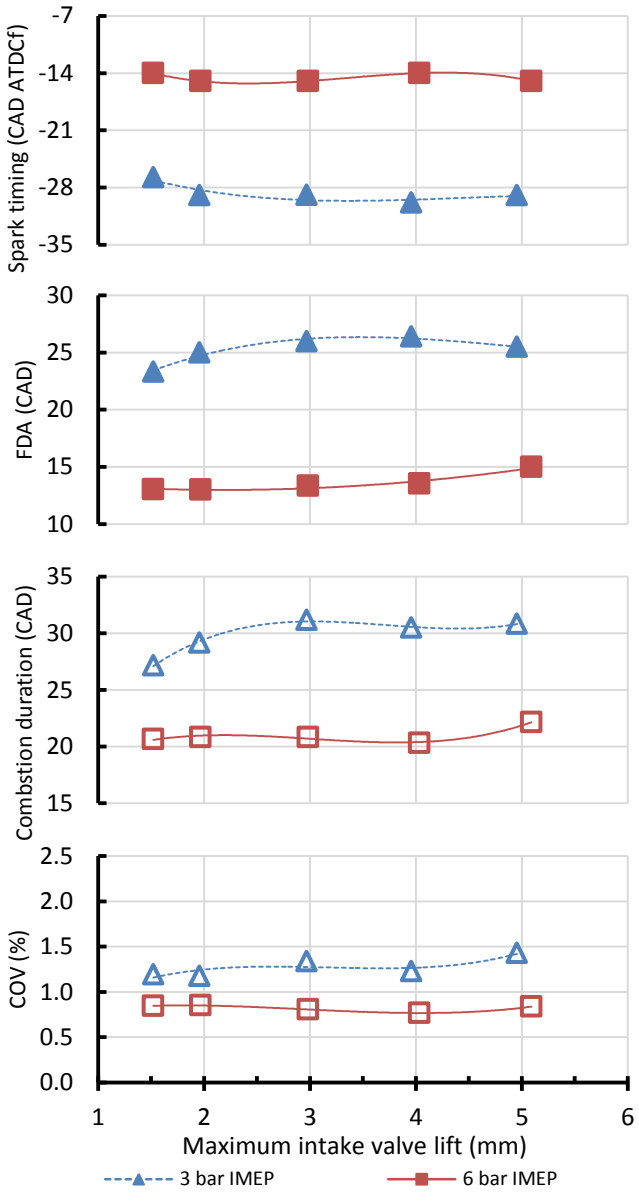

Figure 18. Effect of maximum valve lift in the spark timing, FDA, combustion duration and COV_{imep}.

Some studies suggested that the deactivation of one of the intake valves would generate a higher swirl motion and enhance in-cylinder flow motion resulting in higher turbulence levels prior to spark [14], [16], [12], [15]. In the scenario of this study, such strategy would also delay the IVC and result in increased CR_p. This would produce higher in-cylinder temperatures prior to spark due to the longer compression period, which would be highly beneficial for the low load operation. Even then, the reduction of the flow area from two valves to only one would impair the pumping loop.

The COV_{imep} was relatively low and as expected decreased with the load. As in the lower load FDA and combustion duration increased with the valve lift, there was higher combustion variability which resulted in increase of the COV_{imep} with the valve lift. For the higher load, as higher temperatures were achieved, the combustion process was more stable and the COV_{imep} was almost constant with the increase in valve lift.

Gaseous emissions

Figure 19 presents the gaseous emission data of the 3.1 bar IMEP and 6.1 bar IMEP loads when operating at wide open throttle and using EIVC as load control strategy. There was no clear trend between CO and distinct maximum valve lift. For the lower load, the CO was fairly constant until the lift of 4 mm, and then decreased. For the higher load, there was an increasing trend of CO with valve lift. As the mixture preparation was PFI, these effects were not expected to have a higher influence from the mixing quality. As expected, due to the higher combustion temperature at higher load there was lower CO formation. For the same reason, a higher fraction of ethanol molecules could be broken and oxidized during the higher load combustion process, reducing the THC emissions with the load increment. THC emissions were maintained fairly constant with the increase in the maximum valve lift.

The NOx emissions results were also influenced by the longer combustion process at lower temperature of the higher lift cases. The lower temperature played a major role in reducing NOx emissions as the maximum lift was increased and the effective compression ratio reduced. The increase in load resulted in higher NOx emission as expected.

Efficiency related parameters

Figure 20 presents the effect of the valve lift in the efficiency related parameters. The combustion efficiency was directly related to the emissions. Visibly, the main cause for the decrease in combustion efficiency in the 6 bar IMEP load was the increase of the CO emissions. Even then, the absolute difference between the maximum and the minimum values was around 0.25%, for both loads. In this way, considering all the uncertainties involved in the combustion efficiency calculation, such a small difference would be included in the experiment uncertainty. For this reason, although there was some considerable variation in the CO and THC emissions, the combustion efficiency could be considered constant and would not interfere in the engine operational efficiency.

There was a constant trend in gross thermodynamic efficiency with the increase in the maximum valve lift. This shows that the available energy delivered by the combustion process was not impaired by the maximum intake valve lift.

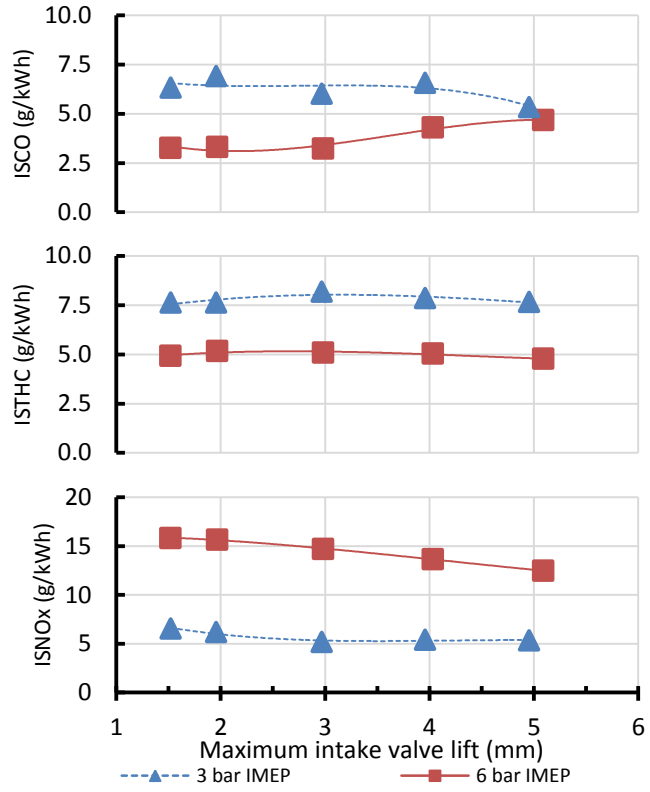

Figure 19. Effect of maximum valve lift in the indicated specific emissions.

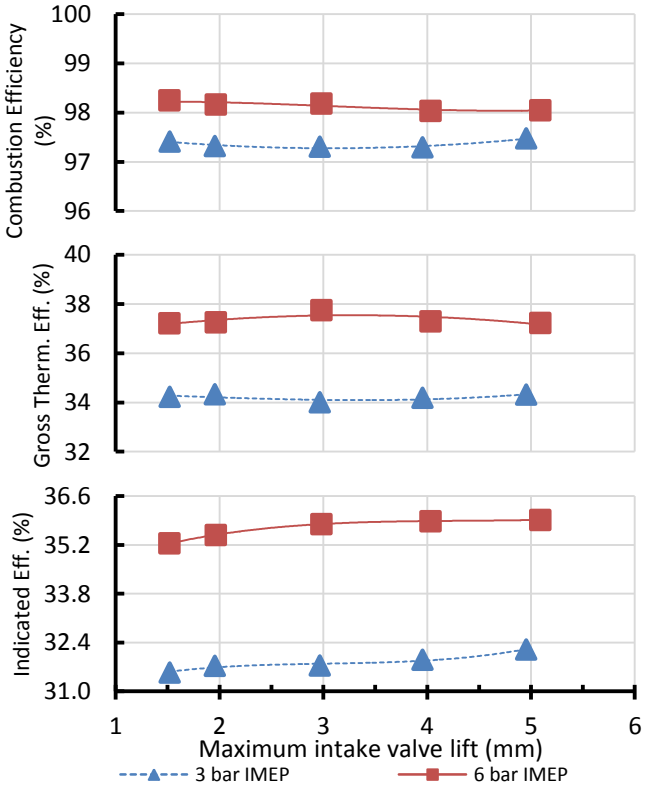

Figure 20. Effect of maximum valve lift in the efficiency related parameters.

The gas exchange efficiency, which varied 1.3% and 2.0% (absolute), for the 3.1 bar IMEP and 6.1 bar IMEP respectively, was the major cause for the indicated efficiency increasing trend with the increase in maximum valve lift. The absolute increase in the indicated efficiency was around 0.7% for both loads, which would represented a relative gain of 2.1% and 1.9% in fuel consumption for the 3.1 bar IMEP and 6.1 bar IMEP loads, respectively.

Discussion and Conclusions

The unthrottled naturally aspirated SI operation with ethanol using EIVC and LIVC load control strategies was studied in order to define which strategy have better potential to increase the engine efficiency. Other effects, as variation of residual gas fraction, were excluded from the analysis as only the IVC was changed.

The EIVC strategy shown the best potential to increase engine efficiency for the all the tested loads at the chosen speed. The main reason was the lower pumping losses. The major drawback of this strategy was the much longer combustion duration at low loads attributed to poor in-cylinder charge motion due to the very early IVC. The major consequence of this effect in real world applications would be the reduced tolerance to cooled EGR. Even then, as for ethanol operation there was no knock tendency, even for the tSI operation strategy, the use of hot EGR would be beneficial in order to delay the IVC moment.

The LIVC strategy presented slightly lower potential to increase engine operating efficiency. The major reason was the higher valve flow loses which increased decreased gas exchange efficiency. Even then, the faster combustion would enable higher EGR tolerance.

The study of the impact of the maximum valve lift in the EIVC operation shown that higher lifts would be desirable in order to reduce flow losses and reduce pumping work. Although the combustion was deteriorated with the increase in maximum valve lift, the gains in the gas exchange efficiency overcame the degradation of the combustion process resulting in net indicated efficiency relative gain of 2.0%.

Finally, the use SI unthrottled operation with ethanol shown good potential to increase engine efficiency. The unthrottled operation would help to reduce the CO_2 emissions by the same amount of the indicated efficiency gains. The addition of the VVA system and its impact in the powertrain consumed power should also be evaluated for real world application.

References

1. E. R. E. C. (EREC), Renewable Energy in Europe: Markets, Trends, and Technologies, Second Ed. London: Earthscan Ltd, 2010.
2. M. R. Maroun and E. L. La Rovere, “Ethanol and food production by family smallholdings in rural Brazil: Economic and socio-environmental analysis of micro distilleries in the State of Rio Grande do Sul,” Biomass and Bioenergy, vol. 63, pp. 140–155, Apr. 2014.
3. The European Union Parliament, “L 140/88,” no. April, pp. 88–113, 2009.
4. A. Walter, P. Dolzan, O. Quilodrán, J. G. de Oliveira, C. da Silva, F. Piacente, and A. Segerstedt, “Sustainability assessment of bio-ethanol production in Brazil considering land use change, GHG emissions and socio-economic aspects,” Energy Policy, vol. 39, no. 10, pp. 5703–5716, Oct. 2011.
5. N. Jeuland, X. Montagne, and X. Gautrot, “Potentiality of Ethanol As a Fuel for Dedicated Engine,” Oil Gas Sci. Technol., vol. 59, no. 6, pp. 559–570, Nov. 2004.
6. K. Nakata, K. Nakata, S. Utsumi, S. Utsumi, 2006, and 2006, “The effect of ethanol fuel on a spark ignition engine,” SAE Tech. Pap., no. 2006013380, 2006.
7. R. A. Stein, C. J. House, and T. G. Leone, “Optimal Use of E85 in a Turbocharged Direct Injection Engine,” SAE Int. J Fuels Lubr., p. 2009011490, 2009.
8. J. Szybist, M. Foster, W. R. Moore, K. Confer, A. Youngquist, and R. Wagner, “Investigation of Knock Limited Compression Ratio of Ethanol Gasoline Blends,” SAE Tech. Pap., no. 20100106, 2010.
9. R. C. Costa and J. R. Sodré, “Compression ratio effects on an ethanol/gasoline fuelled engine performance,” Appl. Therm. Eng., vol. 31, no. 2–3, pp. 278–283, Feb. 2011.
10. P. Kreuter, P. Heuser, and M. Schebitz, “Strategies to improve SI-engine performance by means of variable intake lift , timing and duration,” SAE Tech. Pap., no. 920449, 1992.
11. M. Pischinger, W. Salber, F. Staay, H. Baumgarten, and H. Kemper, “Benefits of the Electromechanical Valve Train in Vehicle Operation,” Sae 2000-01-1223, vol. 2000, no. 724, 2000.
12. S. Diana, B. Iorio, V. Giglio, and G. Police, “The Effect of Valve Lift Shape and Timing on Air Motion and Mixture Formation of DISI Engines Adopting Different VVA Actuators,” SAE Tech. Pap., no. 2001013553, 2001.
13. D. Cleary and G. Silvas, “Unthrottled engine operation with variable intake valve lift , duration , and timing,” SAE Tech. Pap., vol. 2007, no. 724, pp. 2007-01–1282, 2007.
14. P. Stansfield, G. Wigley, C. Garner, R. Patel, N. Ladommatos, G. Pitcher, J. Turner, H. Nuglisch, and J. Heilie, “Unthrottled engine operation using variable valve activation: the impact on the flow field, mixing and combustion.,” SAE Tech. Pap., no. 2007011414, 2007.
15 M. Battistoni and F. Mariani, “Fluid Dynamic Study of Unthrottled Part Load SI Engine Operations with Asymmetric Valve Lifts,” 2009.
16. R. Patel, N. Ladommatos, P. A. Stansfield, G. Wigley, C. P. Garner, G. Pitcher, J. W. G. Turner, H. Nuglisch, and J. Helie, “Un-throttling a direct injection gasoline homogeneous mixture engine with variable valve actuation,” Int. J. Engine Res., vol. 11, no. 6, pp. 391–411, 2010.
17. P. Borgqvist, P. Tunestål, and B. Johansson, “Investigation and Comparison of Residual Gas Enhanced HCCI using Trapping (NVO HCCI) or Rebreathing of Residual Gases,” SAE Pap., no. 2011-01–1772, pp. 925–942, 2011.
18. B. Khalighi, “Intake-Generated Swirl and Tumble Motions in a 4-Valve Engine with Various Intake Configurations-Flow Visualization and Particle Tracking Velocimetry,” SAE Tech. Pap., no. 900059, Feb. 1990.
19. O. Hadded and I. Denbratt, “Turbulence Characteristics of Tumbling Air Motion in Four-Valve S.I. Engines and their Correlation with Combustion Parameters,” SAE Tech. Pap., no. 910478, 1991.
20. S. F. Benjamin, “A phenomenological model for ‘barrel’ swirl in reciprocating engines,” Arch. Proc. Inst. Mech. Eng. Part D J. Automob. Eng. 1989-1996 (vols 203-210), vol. 206, no. 14, pp. 63–71, 1992.
21. K. Y. Kang and J. H. Baek, “Tumble Flow and Turbulence Characteristics in a Small Four-Valve Engine,” SAE Tech. Pap., no. 960265, Feb. 1996.
22. Y. Li, H. Zhao, Z. Peng, and N. Ladommatos, “Analysis of tumble and swirl motions in a four-valve SI engine.,” SAE Tech. Pap., no. 2001013555, 2001.

23. P. G. Hill and D. Zhang, “The effects of swirl and tumble on combustion in spark-ignition engines,” Prog. Energy Combust. Sci., vol. 20, no. 5, pp. 373–429, Jan. 1994.
24. A. Floch, J. Van Frank, and A. Ahmed, “Comparison of the Effects of Intake-Generated Swirl and Tumble on Turbulence Characteristics in a 4-Valve Engine,” SAE Tech. Pap., no. 952457, 1995.
25. T. Urushihara, T. Murayama, K.-H. Lee, and Y. Takagi, “Turbulence and Cycle Variation of Mean Velocity Generated by Swirl and Tumble Flow, and Their Effects on Combustion,” SAE Tech. Pap., no. 950813, 1995.
26. T. Wang, D. Liu, B. Tan, G. Wang, and Z. Peng, “An investigation into in-cylinder tumble flow characteristics with variable valve lift in a gasoline engine,” Flow, Turbul. Combust., vol. 94, no. 2, pp. 285–304, 2015.
27. J.-F. Le Coz, S. Henriot, and P. Pinchon, “An experimental and computational analysis of the flow field in a four-valve spark ignition engine - Focus on cycle-resolved turbulence,” SAE Tech. Pap., no. 900056, 1990.
28. K. Lee, C. Bae, and K. Kang, “The effects of tumble and swirl flows on flame propagation in a four-valve S.I. engine,” Appl. Therm. Eng., vol. 27, no. 11–12, pp. 2122–2130, 2007.
29. I. Bücker, D.-C. Karhoff, M. Klaas, and W. Schröder, “Engine In-Cylinder Flow Control via Variable Intake Valve Timing,” SAE Tech. Pap., no. 2013240055, 2013.
30. M. Dalla Nora, T. Lanzanova, Y. Zhang, and H. Zhao, “Engine Downsizing through Two-Stroke Operation in a Four-Valve GDI Engine,” *SAE Tech. Pap.*, no. 2016010674, 2016.
31. T. D. M. Lanzanova, M. Dalla Nora, and H. Zhao, “Performance and economic analysis of a direct injection spark ignition engine fueled with wet ethanol,” *Appl. Energy*, vol. 169, pp. 230–239, May 2016.
32. T. de Melo, M. de Brito, G. Machado, and C. Paiva, “Procedure for Uncertainty of Measurement Determination of Spark Ignition Engine Emission Tests,” *SAE Tech. Pap.*, no. 2012-36–0488, 2012.
33. R. Munsin, Y. Laoonual, S. Jugjai, and Y. Imai, “An experimental study on performance and emissions of a small SI engine generator set fuelled by hydrous ethanol with high water contents up to 40%,” *Fuel*, vol. 106, pp. 586–592, Apr. 2013.
34. K. Kar, R. Tharp, M. Radovanovic, I. Dimou, and W. K. Cheng, “Organic gas emissions from a stoichiometric direct injection spark ignition engine operating on ethanol/gasoline blends,” *Int. J. Engine Res.*, vol. 11, no. 6, pp. 499–513, Dec. 2010.
35. T. Wallner, “Correlation Between Speciated Hydrocarbon Emissions and Flame Ionization Detector Response for Gasoline/Alcohol Blends,” *J. Eng. Gas Turbines Power*, vol. 133, no. 8, p. 82801, 2011.
36. Economic Commission for Europe of the United Nations, “Regulation No 49 of the Economic Commission for Europe of the United Nations (UN/ECE),” *Off. J. Eur. Union*, no. 171, pp. 1–390, 2013.
37. J. A. Caton, “Combustion phasing for maximum efficiency for conventional and high efficiency engines,” *Energy Convers. Manag.*, vol. 77, pp. 564–576, Jan. 2014.
38. P. Aleiferis, A. Taylor, K. Ishii, and Y. Urata, “The nature of early flame development in a lean-burn stratified-charge spark-ignition engine,” *Combust. Flame*, vol. 136, no. 3, pp. 283–302, Feb. 2004.
39. J. B. Heywood, *Internal Combustion Engine Fundamentals*, 1st ed., vol. 21. McGraw-Hil, 1988.

Acknowledgments

The first would like to acknowledge the Brazilian council for scientific and technological development (CNPq - Brasil) for supporting his PhD studies at Brunel University London.

Contact Information

Thompson D. M. Lanzanova
Brunel University London
lanzanova@gmail.com

Professor Hua Zhao
Brunel University London
hua.zhao@brunel.ac.uk

Definitions/Abbreviations

BDC	Bottom dead center
CA50%	Point of 50% of mass fraction burned
CAD	Crank angle degree
COV_{imep}	Covariance of the IMEP (300 cycles)
CR_p	Effective compression ratio
CR_v	Geometric compression ratio
EGR	Exhaust gas recirculation
EIVC	Early intake valve closure
FDA	Flame development angle
FID	Flame ionization detector
GHG	Greenhouse gases
IMEP	Net indicated mean effective pressure
ISCO	Indicated specific carbon monoxide
ISNOx	Indicated specific nitrogen oxides
ISTHC	Indicated specific total hydrocarbon
IVC	Intake valve closure
LIVC	Late intake valve closure
MBT	Minimum spark advance for the best torque
PMEP	Pump mean effective pressure
SI	Spark ignition
T	Temperature (K)
TDC	Top dead center
THC	Total hydrocarbons
tSI	Throttled spark ignition
V	Cylinder instantaneous volume
Vcc	Combustion chamber volume
Vd	Displacement volume
e	Ethanol fraction in the fuel
k_{FID}	FID correction factor
k_w	Dry to wet correction factor
P_I	Indicated Power
$\dot{m}_{exh}$	Exhaust mass flow rate

u_i	Gas concentration (ppm)	γ	Ratio of specific heats
$[x_i]$	Raw gas exhaust factor	θ	Crank angle

Appendix A

Efficiency related parameters equations

The calculation methodology for the efficiency related parameters is provided below.

Indicated mean effective pressure (net):

$$IMEP = \frac{\int_{-180}^{540} p_i dV}{V_d} \quad (1)$$

where p_i is the instantaneous in-cylinder pressure, V is the instantaneous cylinder volume and V_d is the engine displacement volume.

Indicated efficiency (net):

$$\eta_I = \frac{IMEP.V_d}{m_f.LHV_f} \quad (2)$$

where m_f is the fuel mass flow per cycle and LHV_f is the lower heating value of the fuel.

Pumping mean effective pressure:

$$PMEP = \frac{\int_{EVO}^{IVC} p_i dV}{V_d} \quad (3)$$

Gas exchange efficiency:

$$\eta_{GE} = \frac{IMEP}{IMEP - PMEP} \quad (4)$$

Combustion efficiency:

$$\eta_C = 1 - \frac{\sum \dot{m}_i.LHV_i}{\dot{m}_f.LHV_f} \quad (5)$$

where $\dot{m}_i$is the mass flow rate of the considered exhaust gases as CO, THC and H_2, and LHV_i is their respective lower heating value, while $\dot{m}_f$is the fuel flow rate.

Thermodynamic efficiency (gross):

$$\eta_T = \frac{\eta_I}{\eta_{GE}.\eta_C} \quad (6)$$

Dear reviewers

I would like to thank you in the name of all the authors for all the excellent suggestions and attention given to our manuscript .

The text has been thoroughly reviewed to improve grammatical quality.

It should be noticed that the PMEP calculation methodology has been modified. Previously, it was calculated considering the conventional intake and exhaust phases only (considering firing TDC as “0” CAD, PMEP was calculated from 180 to 540 CAD). The new calculation methodology takes in account the period between EVO and IVC. For this reason there is a difference between the plots of PMEP, gas exchange efficiency and thermodynamic efficiency, in the new and the old versions. Using this methodology the relation between thermodynamic efficiency and indicated efficiency could be better explained.

The reply to the reviewer’s suggestions is provided in the following pages.

Best Regards

Thompson D. M. Lanzanova

PhD candidate

Brunel University London

Answer to Reviewer #: 176576

General Viewable to Author 10/20/2016 11:12:50 AM

This was a well written paper on using different valve closing strategies to control load in an ethanol SI engine. The paper is in good condition as presented and only needs minor corrections for publication

1. Pg 4, in the 2nd paragraph, explain which load the CRv as lower than the CRv, it is not clear from the figures.

For clarification purposes the following text section was added: …"Thus, for the LIVC strategy the CR_v was always smaller (for all loads) than the CR_p.". A text section was also added to clarify the CR_p and CR_p calculation methodologies.

2. In Figure 4 (and 16) the In¬cyli needs to be fixed to In¬cyl

Corrected

3. Pg 6, FDA should be defined somewhere in the paper

"FDA – period between spark and 10% of mass fraction burn" text section is located in the paragraph just before figure 7.

4. Figure 10, there are a few spelling mistakes in the caption

Corrected to: "Figure 10. Average in-cylinder pressure and heat release rate of different valve strategies for 3.1 bar and 6.1 bar IMEP loads."

5. Figure 13, please give the equations used to find the thermodynamic efficiency.

The text section "The calculation procedure used to calculate the efficiency related parameters is provided in appendix A." was included in the Efficiency related parameters section. The appendix A was added to provide the equations used to calculate the efficiency related parameters.

6. Figure 13, Is this the net or gross indicated efficiency? This matters for the conclusions.

It is the net indicated efficiency. The equation is now provided in the Appendix A. Modifications in the text have been made in order to explain the physical meaning of each one of the efficiency parameters evaluated. The gas exchange efficiency and thermodynamic have change from the older version due to the PMEP calculation modification, which now considers the EVO and IVC period.

7. The conclusion about the EIVC being better is not clear to me. It would depend on the above comments on the net or gross efficiency for Figure 13.

In Figure 13, the indicted efficiencies are similar for the EIVC and LIVC, but the pumping is much lower for the LIVC. If Figure 13 is the gross efficiency, then the LIVC should have a higher net efficiency (making it the better choice), but if Fig 13 is the net efficiency, then the EIVC would be better. But this all depends on the experimental error as indicated efficiencies typically have an error of +/¬ 1% so they could really be the same, the authors should include those or comment on the difference in the indicated efficiencies in Figure 13 as the exact difference between the two is hard to tell from the figure and is likely in the range of the experimental uncertainty.

Thank you for the comment. The text has been changed in order to provide a more clear explanation. Due to the change in the PMEP calculation methodology, the relationship between the gross thermodynamic efficiency, gas exchange efficiency and combustion efficiency to the Indicated efficiency became clearer.

It is agreed that the experimental uncertainties would approximate the Ind. Eff. results of EIVC and LIVC. For the lower load cases the minimum relative indicated efficiency difference between LIVC and EIVC cases is around 2%. In this way, even admitting a measurement uncertainty of +-1% (relative value), the trend line would still be higher and the comments would still be valid. For this reason, absolute values are not directly commented in the text when the relative difference is smaller than 3%, only the trends.

A comparison of indicated efficiency gain has been added in the efficiency related parameters section, after figure 13. The comparison was evaluated between each unthrottled operation and tSI. As this difference ranged from 10% to 5% (in the lower load cases), absolute number were used in order to provide a quantitative value.

Answer to Reviewer #: 178669

General Viewable to Author 11/17/2016 04:06:08 PM

Comments on Paper "Investigation of early and late intake valve closure strategies . . . "

1. Would be helpful to define CRv and CRp.CRp is apparent CR which appears to be computed from some measured pressure levels, but not clear.

The second paragraph of the gas exchange sub-section at "Comparative analysis between tSI, EIVC and LIVC" has been modified in order to provide these parameter calculation proceedure:

"As the IVC was varied, the geometric compression ratio, CR_v, deviated from the geometric compression ratio determined by the cylinder volumes at BDC and TDC. CR_v was calculated as the relationship between the TDC in-cylinder volume and volume at IVC. Very low CR_v values were achieved at the lowest loads when using the LIVC strategy. This occurred because the cylinder volume required to trap the amount of air was too small. Due to the valve restrictions and higher in-cylinder pressure required to dispose the excess air back to the intake manifold, an earlier compression phase occurred previously to the IVC event, as shown in Figure 4. Thus, for the LIVC strategy the CR_v was always smaller (for all loads) than the CR_p. The CR_p was calculated as the relationship between the instantaneous in-cylinder volume when a fitted polytropic compression process (fitted to the compression process while all valves were closed) reaches the intake pressure level and combustion chamber volume. Using this approach, the CR_p means the actual compression ratio to which the fluid is subjected starting at the intake pressure state. Figure 4 provides the graphical explanation of the calculation process of CR_p and CR_v. "

2. Also helpful to define gas exchange efficiency. Also a note on difference between indicated efficiency and thermodynamic efficiency. Guess that thermo efficiency is brake work / fuel heating value, whereas indicated effcy is indicated efficiency / fuel heating value.

The Appendix A was added in order to clarify the calculation procedure. Indicated efficiency is the gas work divided by total fuel energy delivered in one cycle. Thermodynamic efficiency was considered as the indicated efficiency divided by combustion efficiency and gas exchange efficiency. In this way, the physical meaning of the thermodynamic efficiency is how well the total fuel energy has been used in the power phase. The division of indicated efficiency by gas exchange efficiency results in the gross indicated efficiency. Dividing again by the combustion efficiency excludes the effects of unburned fuel.

3. Use of lIVC notation in several figures is confusing (Fig 3, Fig 13) is confusing and inconsistent with other figures.Suggest that LIVC be used consistently.

Corrected

4. Confusion in area where effect of valve lift is discussed in paragraph beginning "In order to maintain the desired load." Please review and see if this reads as intended.

The text was modified to "The EIVC had to be adjusted depending on the set maximum valve lift in order to maintain the desired load ".

5. Several word choices are suggested as perhaps being in better agreement with authors intentions:

1. "Assessed" for "accessed" on pg. 3 and several other locations.

Corrected

2. Higher heat of vaporization "decreases" cold start capability, for "increases" on pg. 1.

Corrected

3. Twin "spray" for twin "beam" injector in Table 1.

Corrected

4. Fluid was "subjected" rather than "submitted" on pg. 4.

Corrected through the whole text.

5. "Conversely", in the case of EIVC for "adversely" on pg. 4.

Corrected

6. This effect “required” a higher spark, for “requested” on pg. 5.

Corrected

7. “COV imep” for “COV impe” on pg. 7.

Corrected

8. Valve “seat” for valve “sit” on pg. 9.

Corrected

Answer to Reviewer #: 184234

General Viewable to Author 11/28/2016 01:22:08 AM

This paper investigates the effect intake valve closure timing (early or late) on engine efficiency. It was found that early IVC give higher efficiency compared to late IVC; and higher lift is preferable. The paper is well organized, the experiment method was clear and well executed. However, the paper requires further grammatical check before considering for publication. Besides that, below are several comments that authors could give consideration:

Some figure, it seems curve-fitting was used. I suggest not to use straight lines to connect the data points. If using curve-fitting, please describe the equations.

Thank you for the suggestion. No straight lines were used to connect the data points, as suggested. Second and third order polynomial fit were used as convenient. The following text section "Second and third order polynomial curve fitting was used to connect the data points in the plots for better visualization purpose."

The connection lines have the purpose of showing the parameter trend when this has a physical meaning which may not be only directly related to the load. In the opinion of the authors, the polynomial equations of the evaluated parameters as function of load does not contribute to the discussion of the paper and will not be added.

"The flow losses would be increased in the LIVC case due to the longer period with the intake valves opened [10]." – could you elaborate a little bit more? Maybe explain what they found the reference.

The text was modified to: "The flow losses would be increased in the LIVC case due to the longer period with the intake valves opened, as also stated by [10]. The increased flow losses occur due to the additional backflow process necessary to trap the right charge mass quantity for the desired load. Thus, for the LIVC strategy, valve flow restrictions needed to be surpassed twice in the fresh air trapping event (during the fresh air induction and in the subsequent backflow processes). On the other hand, for the EIVC the valve flow restriction needed to be surpassed only during a minimized period during the induction process when the intake valves were opened."

Legend in Figure 13 for late IVC needs to be corrected

Corrected

It seems with lift greater than 3 mm, no significant change or improvement is expected. Can the author provide a possible reason?

Excluding combustion efficiency and thermodynamic efficiency, the gas exchange efficiency should be evaluated. As there was considerable increase in gas exchange efficiency with the increase of valve lift, the indicated efficiency should also increase. It did not occurred for the 6.1 bar IMEP load due to the decrease in combustion efficiency resultant of the CO increase. This occurred due the manual lambda control (as explained in the text). For the lower load it could be noticed an indicated efficiency relative increase in the order of 1.5%. So, it shows that the impact of the maximum valve lift is bigger at low loads.

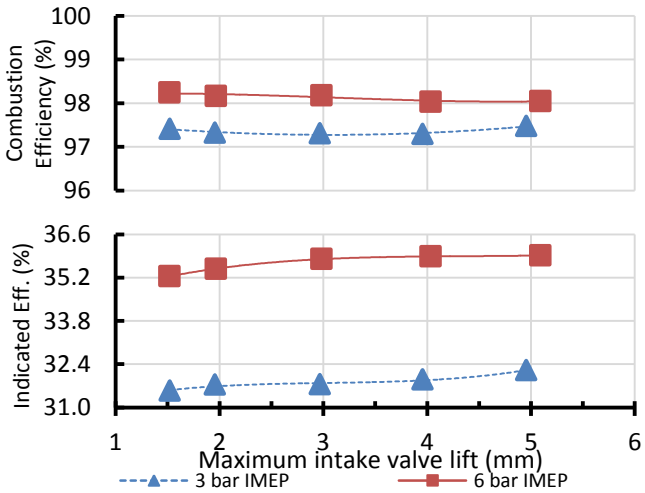

The conclusion would be better if authors could provide specific values were found within the test condition of this study. For example, how much efficiency was improved overall? What was the desirable lift? How much CO2 was reduced under SI unthrottled operation?

In the Efficiency related parameters section of the tSI, LIVC and EIVC comparison the text section has been added to inform the expected fuel consumption gains related to indicated efficiency:“ The tSI case presented the lowest net indicated efficiency especially due to the impaired gas exchange efficiency. If directly translated to real world operation, the unthrottled operation indicated efficiency gains would result in better fuel economy. Thus, it could be expected around 3.7% or 5.9% fuel economy gain when using LIVC or EIVC, respectively, against the conventional tSI (when averaging the net indicated efficiency gains for all loads). Considering only the loads up to 4.5 bar IMEP, the average gain would be 6.5% and 9.2% (for LIVC and EIVC strategies, respectively).”

The following text section presents the relative gains due to maximum valve lift variation: “The absolute increase in the indicated efficiency was around 0.7% for both loads, which would represented a relative gain of 2.1% and 1.9% in fuel consumption for the 3.1 bar IMEP and 6.1 bar IMEP loads, respectively.”

In the conclusion the text section presents the relative gain due to maximum valve lift: “…resulting in net indicated efficiency relative gain of 2.0%.”

As the actual CO_2 emissions are directly linked to the fuel consumption, the gains in indicated efficiency would be expected to be directly translated to CO_2 reduction. Even then, the VVA system impact in the powertrain consumed power should also be evaluated. Once the single cylinder test facility is experimental, it is not possible to correctly estimate this impact. So, the last paragraph of the conclusion text section has been modified to: “Finally, the use SI unthrottled operation with ethanol shown good potential to increase engine efficiency. The unthrottled operation would help to reduce the CO_2 emissions by the same amount of the indicated efficiency gains. The addition of the VVA system and its impact in the powertrain consumed power should also be evaluated for real world applications”.